ORIGINAL CONTRIBUTION

Modified apple polysaccharide regulates microbial dysbiosis to suppress high-fat diet-induced obesity in C57BL/6J mice

Yuhua Li[1,4] · Wenqi Xu[2,3] · Yang Sun[5] · Yan Wang[2,3] · Yuan Tang[4] · Yunhua Li[2,3] · Xiaowei Gao[1] · Can Song[1] · Li Liu[2,3] · Qibing Mei[1]

Abstract

Purpose Obesity, substantially increasing the risk of diseases such as metabolic diseases, becomes a major health challenge. In this study, we, therefore, investigated the effect of modified apple polysaccharide (MAP) on obesity.

Methods Twelve male C57BL/6J mice were given a 45% high-fat diet (HFD) for 12 weeks to replicate an obesity model and six mice were given normal diet as control. Then, 1 g/kg MAP was administrated to six mice by gavage for 15 days. Illumina Miseq PE300 sequencing platform was used to analyze the microbial diversity of fecal samples. Flow cytometry was employed to investigate the effects of MAP on immune cells in adipose tissue. Bacterial culture and qPCR were used to assess the effects of MAP on the growth of whole fecal bacteria and representative microbiota in vitro.

Results MAP could alleviate HFD-induced obesity and decrease body weight of mice effectively. The results of α diversity showed that Shannon index in HFD group was significantly lower than that in control group; Shannon index in MAP group was higher than that in HFD group. The results of β diversity showed that the microbiota of MAP group was more similar to that of control group. HFD increased the number of T cells and macrophages in adipocytes; while MAP decreased the number of T cells and macrophages. MAP could promote the growth of fecal bacteria, and demonstrated a facilitated effect on the proliferation of *Bacteroidetes*, *Bacteroides*, *Lactobacillus*, and an inhibitory effect on *Fusobacterium*.

Conclusions MAP could reduce HFD-induced obesity of mice effectively. The possible mechanisms are that MAP restored HFD-induced intestinal microbiota disorder, downregulated the number of T cells and macrophages in adipose tissue.

Keywords High-fat diet · Obesity · Modified apple polysaccharide · Intestinal microbiota · Inflammation

Abbreviations

BDE	*Bacteroides*
BTE	*Bacteroidetes*
FIR	*Firmicutes*
FUS	*Fusobacterium*
HDL-C	High-density lipoprotein cholesterol
HFD	High-fat diet

Yuhua Li, Wenqi Xu and Yang Sun have contributed equally to this work.

✉ Li Liu
liliu40@live.cn

✉ Qibing Mei
qbmei53@hotmail.com

1. Department of Microbial and Biochemical Pharmacy, School of Pharmacy, Southwest Medial University, Luzhou 646000, Sichuan, People's Republic of China

2. State Key Laboratory of New Drug and Pharmaceutical Process, Shanghai Institute of Pharmaceutical Industry, China State Institute of Pharmaceutical Industry, Shanghai 200437, China

3. Shanghai Professional and Technical Service Center for Biological Material Drug-Ability Evaluation, Shanghai 200437, China

4. Department of Pharmacy, The First Naval Force Hospital of Southern Theatre Command, Zhanjiang 524005, Guangdong, People's Republic of China

5. Key Laboratory of Gastrointestinal Pharmacology of Chinese Materia Medica of the State Administration of Traditional Chinese Medicine, Department of Pharmacology, School of Pharmacy, The Fourth Military Medical University, Xi'an 710032, Shaanxi, People's Republic of China

LDL-C   Low-density lipoprotein cholesterol
LAC   *Lactobacillus*
MAP   Colitis-associated colorectal cancer
TC   Total cholesterol
TG   Triglyceride

Introduction

World Health Organization (WHO) defines obesity as excessive fat accumulation that might damage health and is diagnosed at the body-mass index (BMI) ≥ 30 kg/m^2 [1]. The prevalence of overweight and obese between 1980 and 2013 increased 47.1% for children and 27.5% for adults. A total of 2.1 billion individuals were considered as overweight or obese [2]. According to statistics from NCD Risk Factor Collaboration, the number of obese people in the world rose from 150 million in 1975 to 641 million in 2014 [3].

Obesity is associated with the risk of metabolic diseases (e.g., type 2 diabetes mellitus and fatty liver), cardiovascular diseases (hypertension, myocardial infarction, and stroke), musculoskeletal disease (osteoarthritis), Alzheimer disease, depression, and some kinds of cancer (e.g., breast, ovarian, prostate, liver, kidney, and colon) [4, 5]. Furthermore, obesity might lead to reduced quality of life and social disadvantages [6].

It is a high priority then to reduce the obesity-related burden to health and societies as well as to reverse the increase in obesity prevalence.

In recent years, intestinal microbiota has become a focus of obesity and obesity-associated metabolic phenotypes. Backhed et al. found that normal mice consumed more fat and gained 42% more body fat than aseptic mice [7]. Then, after transplanting aseptic mice with bacteria from the cecum of normal mice, body fat of aseptic mice increased by 60% in 2 weeks, accompanied by insulin resistance, adipocyte hypertrophy, increased leptin, and glucose levels. Therefore, intestinal microbiota plays an important role in the process of body weight change. If the intestinal microecosystem is imbalanced and the composition and proportion of normal microbiota are modified, the occurrence and development of obesity and its metabolic syndrome will be accelerated. Studies have shown that intestinal microbiota imbalance can lead to obesity by transplanting disordered microbiota into sterile mice. Ridaura et al. [8] colonized the fecal microbiota of two genetically identical twins, one fat and one thin, into the intestines of sterile mice fed a low-fat diet, and found that the sterile mice receiving the "fat" microbiota became fat, while the sterile mice receiving the "lean" microbiota remained thin.

During the development of obesity, dysbiosis plays a role through a variety of mechanisms, such as regulating the "brain–gut axis" to increase energy uptake, affecting the metabolites of the microbiota, thereby inhibiting energy metabolism [9]. It seems to be reasonable to control body weight through regulating the gut microbiota.

In our previous study, we found that modified apple polysaccharide (MAP) exerted health benefits through inhibiting gut dysbiosis and chronic inflammation and regulating gut permeability in high-fat diet (HFD)-induced dysbiosis rats [10]. We, therefore, supposed that MAP may play an anti-obesity effect through intestinal microbiota and tried to verify the hypothesis in an HFD-induced obesity model in male C57BL/6J mice.

Materials and methods

Chemicals and reagents

10% low-fat diet and 45% HFD were obtained from Nantong Trophic Animal Feed High-tech Co. Ltd (code: TP23102 and TP23100) (Jiangsu, China); and MAP was extracted as previously described [11].

Induction of a mouse model of obesity

All animal experiments were approved by the Ethical Committee for Animal Care and Use of China State Institute of Pharmaceutical Industry. Eighteen male C57BL/6J mice aged 5 weeks were obtained from Shanghai Xipuer-Bikai Laboratory Animal Co., Ltd. (Shanghai, China), and housed in metabolic cages with a light/dark cycle of 12 h at a temperature of 21 °C ± 1 °C. All possible efforts were made to minimize the animals' suffering and to reduce the number of animals used.

The mice were randomly divided into control group (6 mice) and HFD group (12 mice) before the establishment of the model. Briefly, the experiment was done as previously described [12]. All mice were quarantined for 6 days. At the 7th day, the control group was only given low-fat diet, while the mice in HFD group were given HFD. Each mouse was given an unlimited amount of diet.

At the 12th week, mice in the HFD group were randomly and equally divided into two groups: HFD group, and MAP group [MAP, 1 g (MAP)/kg (body weight)]. The mice in control group were still fed with low-fat diet, while the other groups were still fed with HFD. Treatment with MAP [MAP was dissolved in distilled water to prepare a solution of 0.1 g/mL (w/v)] was administrated by gavage in a dosage of 10 mL/kg every day for 15 days.

Glucose tolerance test (GTT)

At the end of the experiment, the mice were fasting for 16 h but given water ad libitum and then weighed. The tip of tails

of mice was scored using a sterilized blade. A small drop of blood (< 5 μL) was placed on the test strip of the blood glucose meter (Yuyue Medical Equipment Co., Ltd., Jiangsu, China). And the blood glucose was measured as the value of 0 h. The mice were then intraperitoneally administered with 50% glucose solution (4 mL/kg), and the blood glucose values at the points of 15, 30, 60, 90, and 120 min were collected, respectively. The time curve of blood glucose level was made to compare the differences of glucose tolerance between groups.

Serum biochemical analysis

Approximately 500 μL blood were collected from the inner canthus of mice and placed for half an hour, and then centrifuged at 3500 rpm for 10 min to obtain serum. 150 μL serum were immediately measured by 7080 biochemistry automatic analyzer (HITACHI, Tokyo, Japan) to detect the level of total cholesterol (TC), triglyceride (TG), low-density lipoprotein cholesterol (LDL-C), and high-density lipoprotein cholesterol (HDL-C).

Collection of adipose tissue

On the day before dissection, the mice were fasting. Then, the mice were euthanized by ether overdose. And adipose tissue of epididymis and perirenal adipose tissue were removed to weigh. 0.5 g of adipose tissue of epididymis per mouse was fixed with 10% formaldehyde. Hematoxylin–eosin (HE) staining was performed on 10% formaldehyde-fixed epididymal adipose tissue samples after paraffin section.

DNA extraction

Briefly, at the end of the experiment, five independent fecal samples per mouse were collected and fecal bacteria and bacterial DNA were extracted. The fecal samples were re-suspended with 4 mL PBS. Thirty min later, the upper suspension was transferred to another sterilized centrifugal tube. The transferred suspension was centrifuged at $200g$ for 10 min to further remove impurities and then transferred to another sterilized 15 mL centrifugal tube and centrifuged at $3220g$ for 5 min to obtain fecal bacteria, which were then suspended with 0.6 mL TE buffer. 20 μL lysozyme (200 mg/mL, prepared with TE) were added, incubated at 37 °C for 3 h, and then, 70 μL of 10% SDS and 15 μL of proteinase K (20 mg/mL, prepared with TE) were added, and incubated overnight at 55 °C. DNA was extracted by phenol–chloroform–isoamyl alcohol (25:24:1) solution, centrifuged for 10 min at $12,000g$, and then transferred to another EP tube. DNA was precipitated at 4 °C for 30 min with 0.1 times 3 M sodium acetate (pH 5.2) and 0.6 times volume of isopropanol. The precipitated DNA was collected by centrifuging

at $12,000 \times g$ for 10 min. DNA was washed with 70% ethanol, vacuum dried, and dissolved in 0.2 mL TE buffer. OD_{260}/OD_{280} of the DNA was detected by Beckman DU-800 Coulter (CA, USA). The values of 1.8–1.9 were regarded as qualified.

Sequencing analysis of fecal microbiota diversity in mice

DNA samples from mouse feces were amplified by PCR and sequenced for microbial diversity by Shanghai Majorbio Co., Ltd. The primers for PCR amplification were 338F-806R (V3–V4 variable region of 16sRNA gene) with barcode. The sequence of primers was as follows: 338F 5′-ACTCCTACGGGAGCAGGCAG-3′ and 806R 5′-GGACTACHVGGGTWTCTAAT-3′. The PCR reaction system was: FastPfu buffer 4 μL, dNTPs 2 μL, primers 0.8 μL, TransStart®FastPfu DNA polymerase (TransGen Biotech, Beijing, China) 0.4 μL, and DNA template 10 ng, supplemented with double steamed water to 20 μL. The conditions of PCR reaction were as follows: (1) 95 °C 3 min; (2) a: 95 °C 30 s; b: 55 °C 30 s; c: 72 °C 45 s, in a total of 27 cycles; (3) 72 °C 10 min. PCR products were detected by 2% agarose gel electrophoresis. The products were recovered by DNA gel Recovery Kit (Corning, NY, USA). PCR products were detected by QuantiFluor™-ST blue fluorescence quantitative system (Promega Corporation, Madison, WI, USA). According to the sequencing requirements of each sample, the products were mixed according to the corresponding proportions. Illumina platform library was constructed and sequenced by Illumina Miseq PE300 sequencing platform. Operational taxonomic units (OTUs) with sequence similarity over 97% were analyzed. The taxonomy of each 16S rRNA gene sequence was analyzed using RDP classifier (http://rdp.cme.msu.edu/) against the SILVA ribosomal RNA gene database using a confidence threshold of 70% [13, 14].

Flow cytometric analysis

Two hundred mg epididymal adipose tissue samples of each mouse were digested at 37 °C for 30 min with 1 mg/mL collagenase I and centrifuged for 5 min at $500g$, and then, the cell pellets were re-suspended and filtered through a 70 μm cell strainer, washed with ice cold PBS three times, and centrifuged for 5 min at $500g$. The supernatant was discarded and precipitated with ACK lysis buffer for 10 min and centrifuged for 5 min at $500g$. The supernatant was discarded again, and the precipitated cells were re-suspended with PBS and then counted. The cell density was adjusted to 2×10^6/mL. According to the volume ratio of 1:200, the corresponding antibodies (anti-mouse CD3 FITC and anti-mouse F4/80 FITC, Thermo Fisher Scientific, Waltham, MA

USA) were added and incubated in the dark for 30 min, and then detected and analyzed by flow cytometry using a Cytoflex S flow cytometer (Beckman Coulter, CA, USA).

Growth of fecal bacteria in vitro

The bacteria isolated from the feces of control mice were divided into three groups: 1% MAP, 1% MAP + fecal bacteria and fecal bacteria. The fecal bacteria were cultured in basic carbon-free medium (50 mM sodium hydrogen phosphate, 50 mM potassium dihydrogen phosphate, 25 mM ammonium sulfate, and 2 mM magnesium sulfate) with or without 1% MAP. After 48 h of incubation in anaerobic chamber, the precipitation of each group of bacteria was observed, and the concentration of bacterial DNA was extracted to observe the change of bacterial number.

Growth curve of whole fecal microbiota in vitro

The fecal bacteria were diluted 1000 times with basic carbon-free medium and transferred into 15 mL centrifugal tubes. The bacteria were divided into 2% glucose, 2% galactose, 0% MAP, 0.25% MAP, 0.5% MAP, and 1% MAP groups, and then cultured in a bacterial incubator. The OD_{630} was determined with 200 μL of the bacterial solution at different times.

Detection of representative bacteria in MAP-incubated fecal microbiota by qPCR

Our previous studies showed that MAP could affect the intestinal microbiota of *Bacteroides* (BTE), *Bacteroides* (BDE), *Lactobacillus* (LAC), *Firmicutes* (FIR), and *Fusobacterium* (FUS). And then, the effect of 1% MAP on these five microbiotas in vitro was investigated by qPCR. The primers used were demonstrated in Table S1. The PCR reaction system was: SYBR Green premix (Tiangen Biotech (Beijing) Co. Ltd. Beijing, China) 12.5 μL, primers 2 μL, and DNA template 1 μL, ddH$_2$O 9.5 μL. The conditions of PCR reaction were as follows: (1) 95 °C 30 s; (2) a: 95 °C 5 s; b: 60 °C 20 s; c: 72 °C 30 s, in a total of 40 cycles; (3) a: 95 °C 60 s; b: 55 °C 30 s; c: 95 °C 30 s.

Statistical and ecological analysis

Statistical differences among control, HFD, and HFD + MAP treatment groups were analyzed using one-way analysis of variance (ANOVA) followed by a post hoc multiple comparisons using Fisher's least significant difference (LSD) *t* test. Probability (*P* value) of less than 0.05 was regarded as statistically significant.

Alpha-diversity analyses, including community diversity parameter (Shannon), were calculated using the mothur

software [15]. Beta diversity measurements, including gut microbiota trees, were calculated as described [16], and principal coordinate analyses (PCoA) based on OTU compositions were determined. Bacterial taxonomic distributions of sample communities were visualized using the R package software.

Effects of MAP on body weight and food intake in HFD-induced obese mice

As shown in Fig. 1a, after being fed with HFD for 4 weeks, the body weight of mice in HFD group increased significantly when compared with those in control group and lasted until 12 weeks (*P* < 0.05).

The body weight of mice in MAP group decreased significantly, which was similar to that of control group on the 15th day of administration, with significant difference when compared with that of HFD group (*P* < 0.01) (Fig. 1b, c).

In comparison to that of HFD group, MAP treatment made the mice eat less on the 9th and 12th day (*P* < 0.05) (Fig. 1d).

Effects of MAP on adipocytes morphology and liver pathology, fat index, and blood lipid and glucose metabolism in HFD-induced obese mice

HE staining (Fig. 2a–c) showed that compared with that of control group, the size of adipocytes of mice in HFD group increased; after 15 days of MAP intervention, the size of adipocytes decreased, which was similar to that of control group.

Figure 2d–f demonstrates that there were several large fat vacuoles in the liver of HFD-treated mice; while just only a few small fat vacuoles were observed in mice liver of MAP group.

The results of fat index [adipose tissue/body weight (g/100 g)] (Fig. 3a) showed that the weight of epididymal adipose tissue (*P* < 0.01) and perirenal adipose tissue (*P* < 0.01) of HFD-treated mice increased significantly compared with those of control group; 15 days of MAP treatment decreased epididymal adipose tissue (*P* < 0.01), and perirenal adipose tissue significantly (*P* < 0.05).

Figure 3b and c shows that the serum TC level of mice in HFD group increased significantly (*P* < 0.01) and HDL-C/TC level decreased significantly (*P* < 0.05) compared with those of control group. Fifteen days of MAP treatment decreased the TC level (*P* < 0.01) and the TG level (*P* < 0.05), and let the HDL-C/TC level return to the same level as that of control group (*P* < 0.05).

The results of GTT (Fig. 3d) showed that the blood glucose level of mice in HFD group was higher than that of control group at the time points of 30 and 90 min after administration of 50% glucose (*P* < 0.05). The blood glucose level
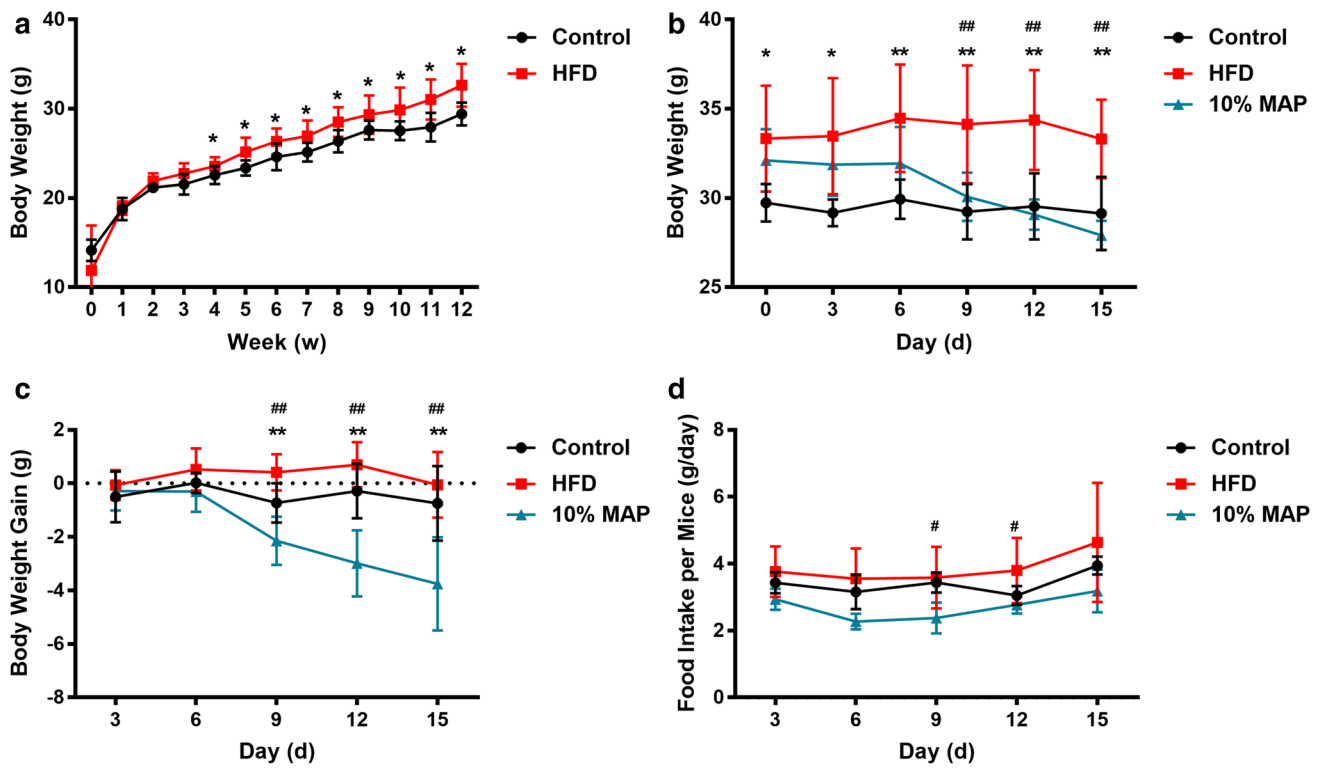
Fig. 1 The effect of MAP on the body weight and food intake of HFD-induced obesity mice (mean ± SD, $n = 6$). **a** Body weight changes of mice during the construction of HFD-induced obesity mice model; **b** body weight changes after MAP treatment; **c** changes of body weight gain after MAP treatment; **d** average food intake after MAP treatment. $*P < 0.05$ vs control; $**P < 0.01$ vs control; $^{\#}P < 0.05$ vs HFD; $^{\#\#}P < 0.01$ vs HFD
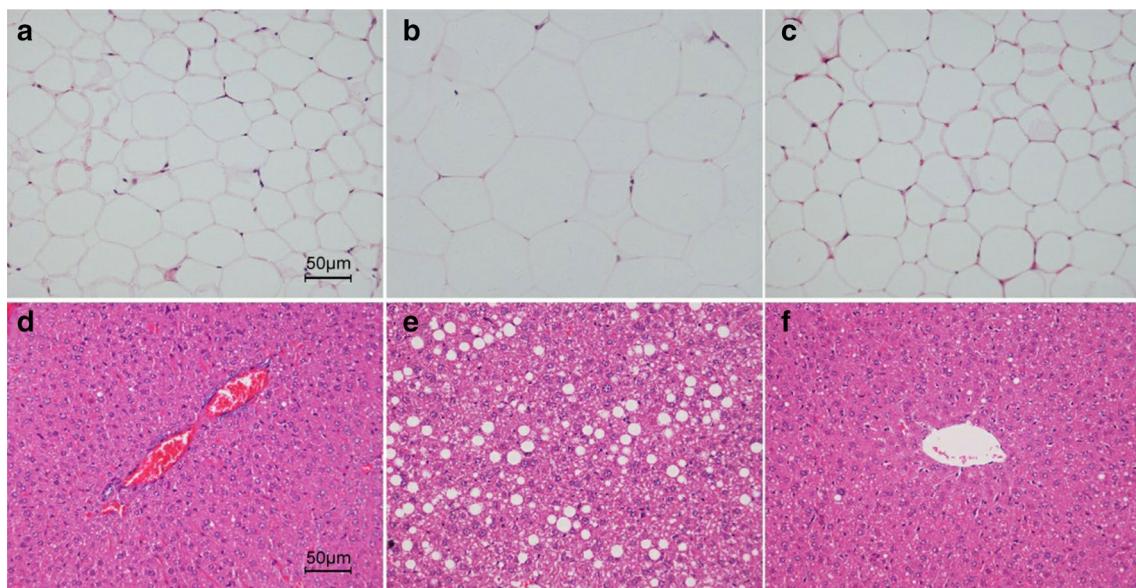

Fig. 2 HE staining of adipose tissue (**a**–**c**) and liver (**d**–**f**) of HFD-induced obesity mice after MAP treatment ($n = 6$). **a**, **e** Control; **b**, **f** HFD; **c**, **g** MAP

of mice in HFD group was also higher than that of control group at other time points; the blood glucose level of mice in MAP-treated group had no significant difference when compared with that of control group.
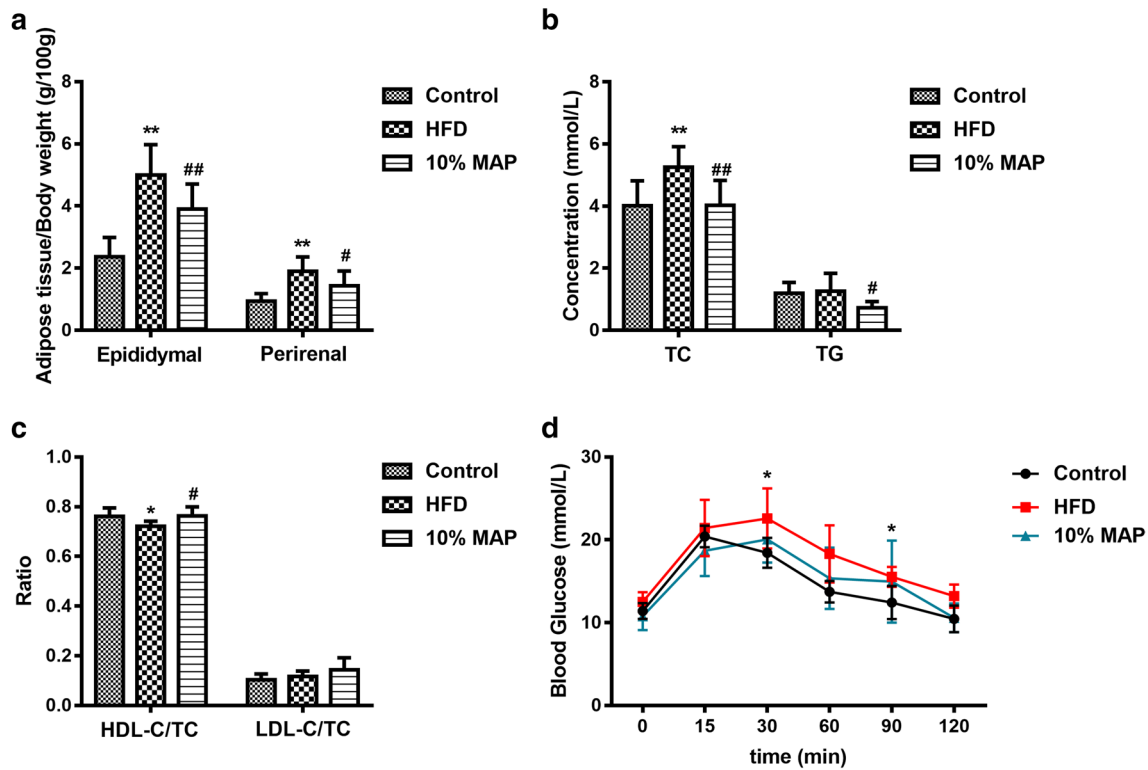
Fig. 3 The effects of MAP on the adipose tissue index, serum lipid levels, and glucose metabolism of HFD-induced obesity mice (mean ± SD, $n=6$). *$P<0.05$ vs control; **$P<0.01$ vs control; #$P<0.05$ vs HFD; ##$P<0.01$ vs HFD

Diversity analysis of α and dilution curve analysis

Shannon index is one of the commonly used indices to evaluate microbial alpha diversity. The larger the Shannon index is, the higher the diversity of the sample community is. The dilution curve is constructed by Shannon index of each sample at different sequencing depths. The community composition of each group was analyzed at the phyla and genus levels. The gentle dilution curve (Fig. 4 and Table 1) indicates that the amount of sequencing data are sufficient to reflect the diversity of most microorganisms in the sample. The results showed that the microbial dilution curves of
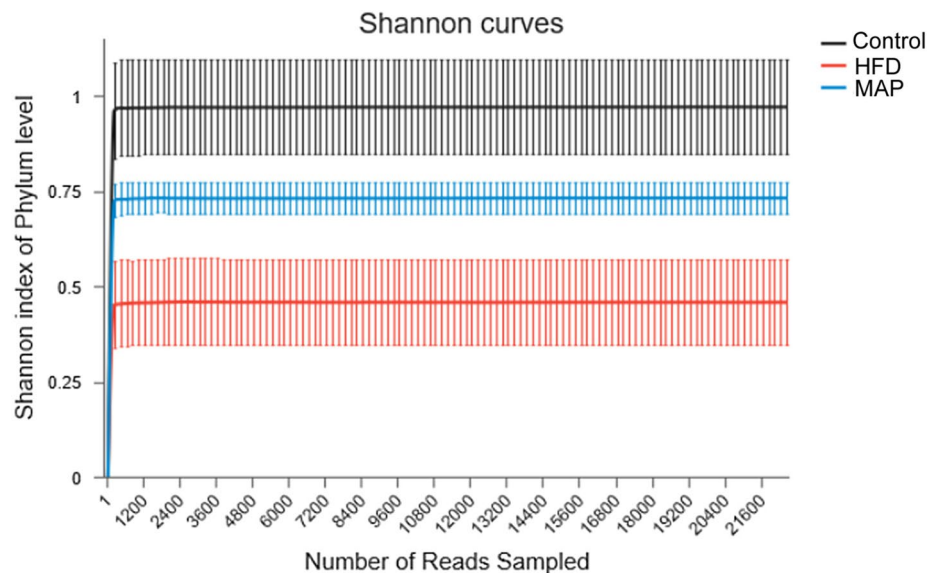
Fig. 4 Rarefaction curve of gut microbiota

Table 1 Shannon index of gut microbiota (mean ± SD)

Group	Shannon index
Control	0.97 ± 0.15
HFD	0.46 ± 0.14*
MAP	0.73 ± 0.05#

*$P < 0.05$ vs control; #$P < 0.05$ vs HFD

intestinal tract of mice in each group tended to be flat with the increase of sequencing depth, indicating that the amount of sequencing data met the requirements. The dilution curve also showed that the intestinal microbial diversity of mice in HFD group was significantly reduced compared with that in control group. MAP intervention could restore the intestinal microbial diversity of mice to a certain degree.

Diversity analysis of β

Sample microbial β diversity was analyzed by sample hierarchical cluster analysis and principal co-ordinates analysis (PCoA). Sample hierarchical cluster analysis (Fig. 5a, b) showed that control group and HFD group belonged to two clusters. MAP group had higher similarity with the control group at the phyla level and genus level.

PCoA analysis (Fig. 5c) showed that the intestinal microorganisms of mice in HFD group were significantly different from those of control group. The intestinal microorganisms of mice in MAP group were different from those of HFD group on the PC1 axis and closer to those of control group.

The results of β diversity (Fig. 5d) showed that MAP could regulate intestinal microorganisms in HFD-induced obese mice and made them close to those of control mice.

Community composition analysis

The results (Fig. 5e and Table 2) showed that *Firmicutes* and *Bacteroides* were two major phyla in the intestinal tract of mice. Compared with those of control group, the abundance of *Firmicutes* in the intestinal tract of mice in HFD group increased significantly and the abundance of *Bacteroides* decreased significantly ($P < 0.05$). Compared with those of HFD group, the abundance of *Firmicutes* in intestinal tract of mice in MAP group decreased significantly ($P < 0.01$), and the abundance of *Bacteroides* increased significantly ($P < 0.01$). After the intervention of MAP, the abundance of intestinal microorganisms in intestinal tract of mice restored to the same level as that in the control group.

At genus level (Fig. 5f and Table 3), compared with those of control group, the abundance of *Lachnospiraceae_NK4A136_group*, *unclassified_f__Lachnospiraceae, Anaerotruncus*, and *Lachnospiraceae_UCG-006* increased, and the abundance of *norank_f__Bacteroidales_S24-7_group* and *Parvibacter*

decreased in HFD group ($P < 0.05$ or $P < 0.01$). Compared with those of HFD group, the abundance of *norank_f__bacteroidales_S24-7_group*, *Bacteroides*, and *unclassified_o__bacteroidales* increased and the abundance of *Intestinimonas* decreased in MAP group ($P < 0.05$ or $P < 0.01$).

Effects of MAP on T cells and macrophages in adipose tissue of HFD-induced obese mice

Flow cytometric analysis (Fig. 6) showed that compared with control group, the number of CD3$^+$ T cells ($P < 0.05$) and F4/80$^+$ macrophages ($P < 0.01$) in adipose tissue of HFD group increased; Compared with HFD group, the number of CD3$^+$ T cells ($P < 0.001$) and F4/80$^+$ macrophages ($P < 0.05$) in adipose tissue of MAP group decreased.

Effect of MAP on the growth of fecal bacteria in vitro

After 48 h of incubation in anaerobic tank, the results showed that there was no sediment at the bottom of the tube in 1% MAP alone, a large amount of sediment at the bottom of the tube in 1% MAP culture, and a small amount of sediment at the bottom of the tube in the control tube (0% AP) (Fig. 7a). MAP can be utilized by the whole fecal bacteria to a certain extent and promoted the growth of fecal bacteria. In addition, bacterial DNA was extracted from each treatment group, and DNA concentration in 1% AP treatment was significantly higher than that in 0% AP treatment ($P < 0.05$) (Fig. 7b).

Effect of MAP on the growth curve of whole fecal microbiota

The results of growth curve test (Fig. 8) showed that the number of bacteria gradually increased after incubation for 32 h, and the growth curve moved up compared with that of 0% MAP. After incubation for 71 h, the bacteria density reached a stable state.

Effect of MAP on representative microbiota

The results of qPCR (Fig. 9) showed that the levels of BTE ($P < 0.05$), BDE ($P < 0.01$), and LAC ($P < 0.01$) in fecal microbiota incubated by 1% MAP in vitro were significantly higher than those in the control group, while the levels of *FUS* ($P < 0.05$) were significantly lower than those in the control group.

Discussion

Obesity is the cause of many chronic diseases such as diabetes, cardiovascular disease, cancer, and so on. With the improvement of living standards, people consume more
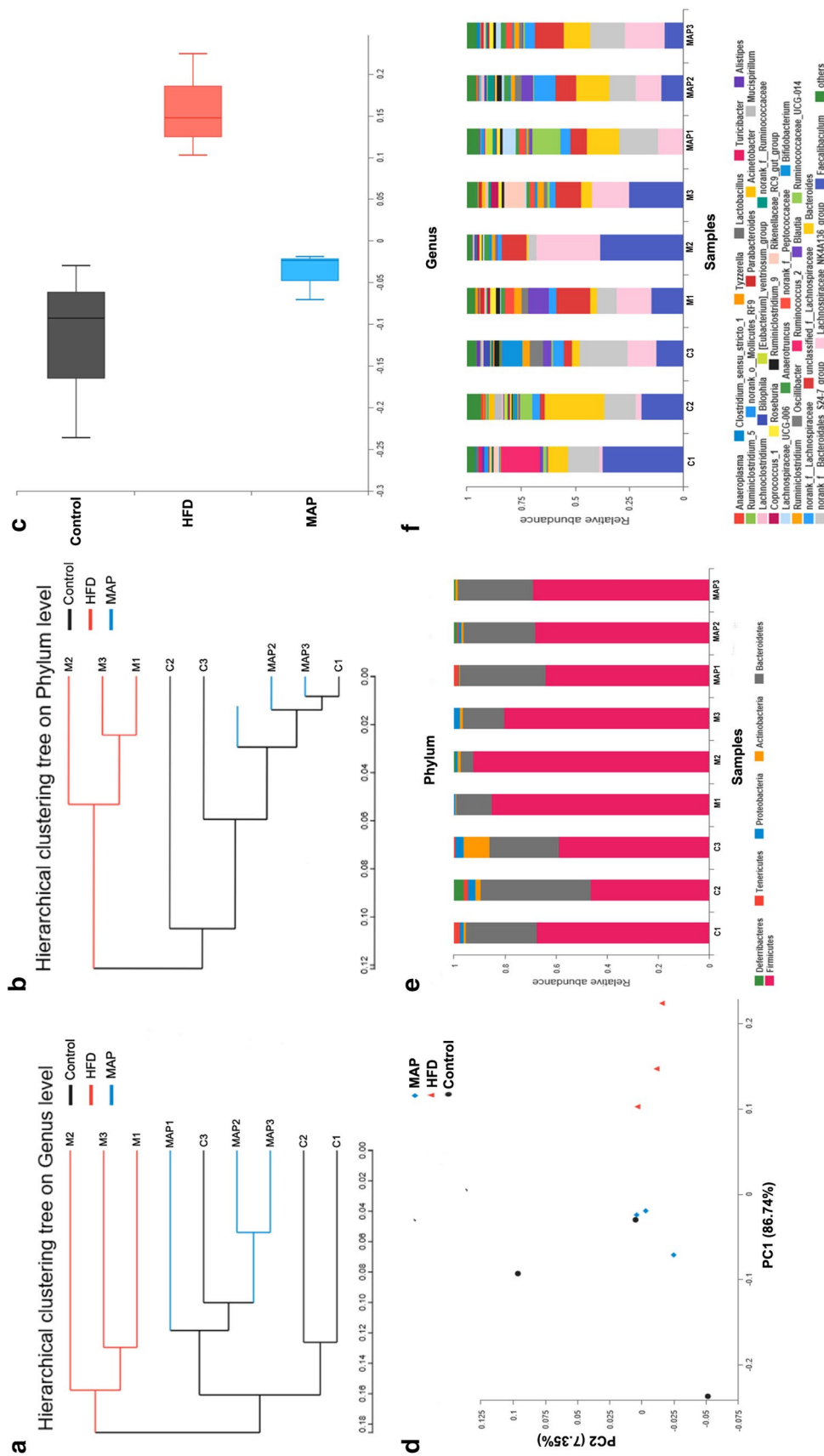
Fig. 5 Sequencing analysis of intestinal microbiota diversity. **a**, **b** Hierarchical clustering analysis of gut microbiota on genus and phyla level. **c**, **d** PCoA of gut microbiota. **e** Composition at phyla level of gut microbiota. **f** Composition at genus level of gut microbiota

Table 2 Composition difference test at phylum level of gut microbiota (mean ± SD, unit: %)

Group	Firmicutes	Bacteroidetes
Control	57.83 ± 10.67	32.86 ± 9.02
HFD	86.31 ± 6.06*	11.69 ± 6.00*
MAP	67.41 ± 2.67##	30.41 ± 2.84##

*$P < 0.05$ vs control; ##$P < 0.01$ vs HFD

energy than they need. Obesity has become a major health problem that troubles people. According to statistics, the number of obese people in China has surpassed that in the United States ranking the first in the world, with 43.2 million obese men and 46.4 million obese women [3]. However, only orlistat is approved by China Food and Drug Administration for clinical use in anti-obesity treatments, which is far from meeting the needs of the market. The use of anti-obesity drugs has also been limited because of a lack of efficacy, poor long-term adherence rates and serious adverse effects.

In recent years, with the development of intestinal microbiota research, improving obesity by regulating intestinal microbiota has become a new research and development hotspot. The microbiota is a major player in energy harvest and storage, as well as in a variety of metabolic functions, including fermenting and absorbing undigested carbohydrates or providing vitamins and amino acids for the host [17].

Table 3 Composition difference test at genus level of gut microbiota (mean ± SD, unit: %)

Group	Control	HFD	MAP
norank_f__Bacteroidales_S24-7_group	17.120 ± 4.308	4.332 ± 4.652*	15.510 ± 3.153#
unclassified_f__Lachnospiraceae	2.260 ± 1.793	12.910 ± 2.446**	10.520 ± 2.967
Bacteroides polymorpha	13.410 ± 12.470	3.042 ± 2.134	14.000 ± 1.754##
Intestinimonas	0.279 ± 0.336	0.727 ± 0.088	0.308 ± 0.134#
unclassified_o__Bacteroidales	0.411 ± 0.268	0.024 ± 0.021	0.326 ± 0.113#
Parvibacter	0.126 ± 0.068	0.002 ± 0.003*	0.005 ± 0.005

*$P < 0.05$ vs control; **$P < 0.01$ vs control; #$P < 0.05$ vs HFD; ##$P < 0.01$ vs HFD
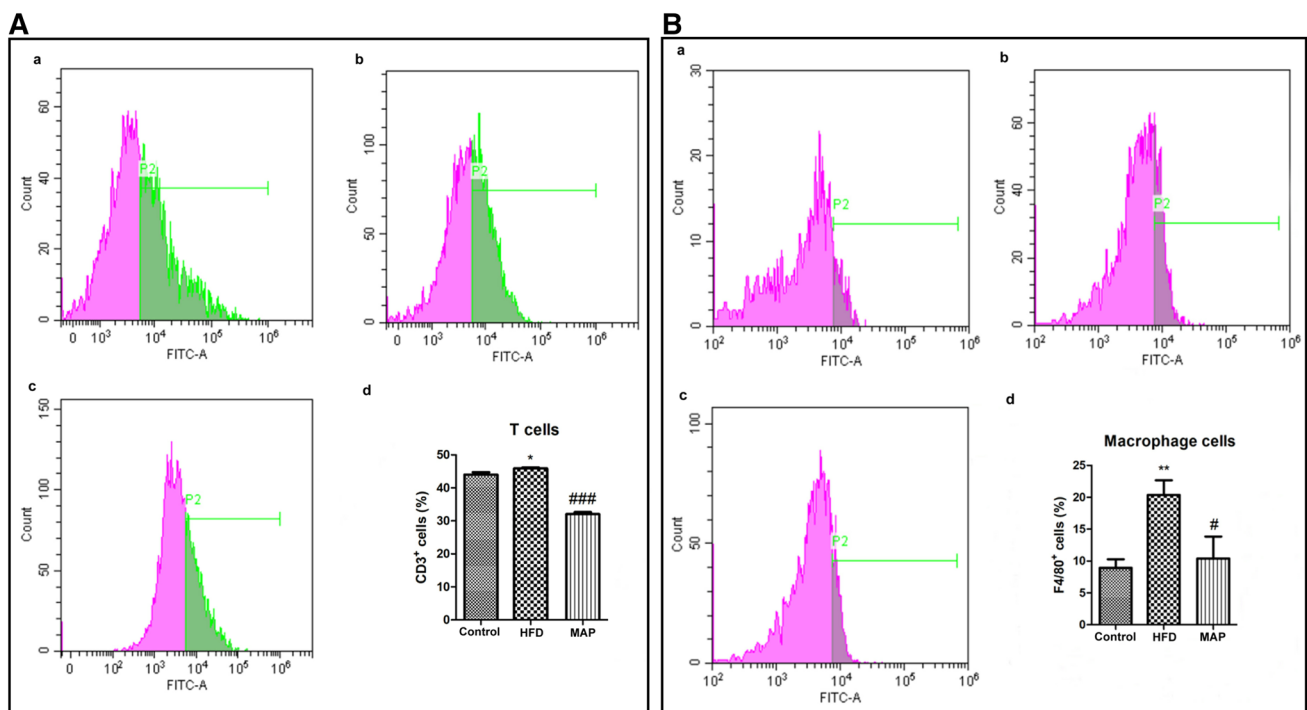

Fig. 6 The effect of MAP on the ratio of T cells and macrophage cells in adipose tissue of HFD-induced obesity mice. **a** The effect of MAP on the ratio of T cells. **a** Control, **b** HFD; **c** MAP; **d** ratio of CD3+ cells of all groups. *$P < 0.05$ vs control; ###$P < 0.001$ vs HFD. **b** The effect of MAP on the ratio of macrophage cells. **a** Control; **b** HFD; **c** MAP; **d** ratio of F4/80+ cells of all groups. **$P < 0.01$ vs control; ##$P < 0.01$ vs HFD
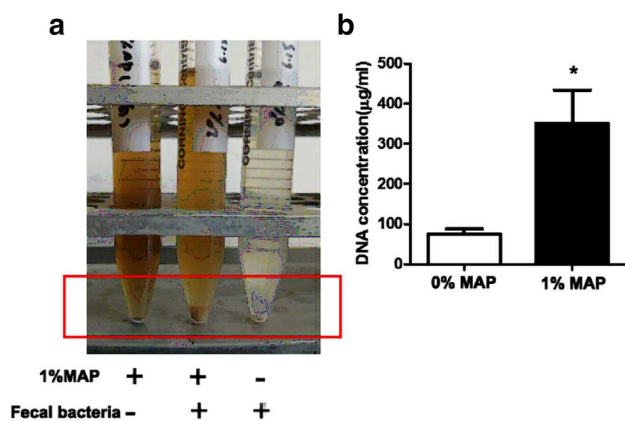
Fig. 7 The effect of MAP on the growth of fecal bacteria. **a** General observation of the effect of MAP on the proliferation of fecal bacteria; **b** DNA concentration of fecal bacteria. (mean ± SD, $n = 3$). *$P < 0.05$ vs control
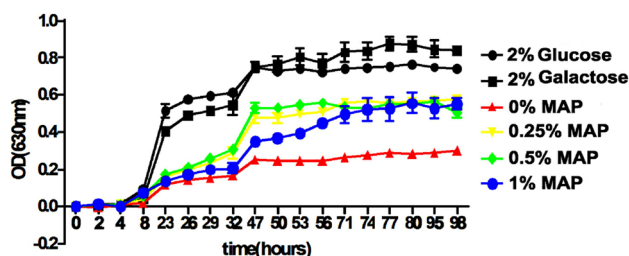

Fig. 8 The effect of MAP on the growth curve of fecal microbiota (mean ± SD, $n = 3$)
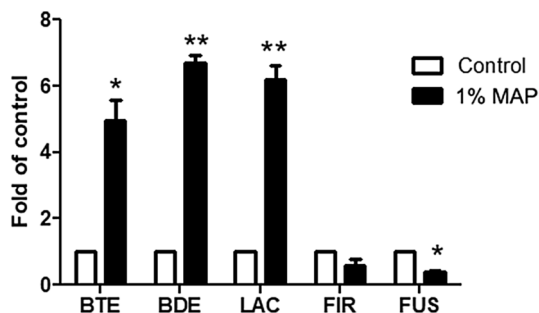

Fig. 9 The effect of MAP on the representative bacteria in feces in vitro (mean ± SD, $n = 3$). *$P < 0.05$, **$P < 0.01$ vs control

Ridaura et al. [8] found co-housing mice harboring an obese twin's microbiota (Ob) with mice containing the lean co-twin's microbiota (Ln) prevented the development of increased body mass and obesity-associated metabolic phenotypes in Ob cagemates, suggesting that dysregulation of bacterial microbiota could enhance obesity. Studies have demonstrated that a *Bifidobacterium CECT 7765* can reduce serum cholesterol and TG in mice fed with HFD,

improve insulin resistance, regulate macrophage and dendritic cell function, and reduce inflammation. Chang et al. [18] found that *Ganoderma lucidum* water extract can reduce body weight, metabolic endotoxemia, and insulin resistance by regulating intestinal microbiota disturbance and barrier function in HFD-treated mice. In the current study, we found that MAP could reduce HFD-induced obesity in mice, decrease lipid accumulation in adipose tissue and liver, and improve blood lipid level. MAP can significantly regulate intestinal microbiota imbalance induced by HFD, restore the disordered intestinal microbiota to a similar level as that of control group, and reduce the number of T cells and macrophages in adipose tissue.

Two groups of beneficial bacteria are dominant in the human gut, the *Bacteroidetes* and the *Firmicutes*. The proportion of *Bacteroidetes* is decreased in obese people when compared with lean people, while this proportion increases with weight loss [19]. The relative abundance of the two predominant bacterial divisions in mice differs between lean and obese animals: mice that are genetically obese have 50% fewer *Bacteroidetes*, and correspondingly more *Firmicutes*, than their lean siblings [20]. MAP incubation in vitro can promote the growth of isolated normal fecal microbiota and can be used by isolated normal fecal microbiota. The results of qPCR showed that the number of *Bacteroidetes* (BTE), *Bacteroides* (BDE), and *Lactobacillus* (LAC) increased significantly in 1% MAP incubation group compared with 0% MAP incubation group ($P < 0.01$). The number of *Fusobacterium* (*Fus*) decreased significantly ($P < 0.05$). In parallel with the observation in vitro, the abundance of *Firmicutes* in intestinal tract of MAP-treated mice decreased ($P < 0.01$), and the abundance of *Bacteroides* increased significantly ($P < 0.01$) (Figs. 4, 5e and Table 1), suggesting that MAP may improve HFD-induced obesity, at least in part through regulating the proportion of the *Bacteroidetes* and the *Firmicutes.*

Evidences show that the microbiota may impact weight gain and adiposity via several inter-connected pathways, including energy harvest and production of microbial metabolites, through effects on inflammatory responses and on the gut–brain axis.

One of the most important metabolic activities of microbiota is the production of short-chain fatty acids (SCFAs) (acetate, propionate, and butyrate), through fermentation of microbiota accessible, complex carbohydrates (MAC) (e.g., oligosaccharides, resistant starch, and plant cell wall materials) [21–23]. Absorbable SCFAs are important modulators of gut health and immune function [24], intestinal hormone production, and lipogenesis [25]. SCFAs can bind to G protein-coupled receptors GPR41 and GPR43 to stimulate the secretion of appetite-suppressing hormones such as glucagon-like peptide 1 (GLP-1), PYY, and cholecystokinin (CCK), which can directly affect the hypothalamic nucleus

group to reduce the activity of NPY/AgRP neurons, activate POMC neurons, and stimulate the appetite center to send a satiety signal to reduce appetite. When the intestinal microbiota is disturbed and the level of endocrine hormones changes, it will affect the appetite center and lead to excessive energy intake, eventually leading to obesity. Psichas et al. [26] found that propionic acid can stimulate intestinal secretion of PYY and GLP-1, thereby inhibiting food intake in mice. Perry et al. [27] confirmed that after HFD modified intestinal microecology, the amount of acetic acid in intestine and plasma increased significantly, parasympathetic nervous system was activated, and insulin and ghrelin secretion increased, which stimulated appetite and induced obesity. SCFAs do not only play an important role in the process of energy intake, but also are indispensable in energy metabolism. The combination of SCFAs and G protein-coupled receptor 43 (GPR43) can inhibit the activity of adenylate cyclase (AC), suppress the conversion of ATP to cAMP, thus increasing the ratio of ATP to cAMP, and lead to the dephosphorylation of hormone-sensitive lipase (HSL), resulting in the reduction of fat decomposition in white adipose tissue and ultimately the reduction of free fatty acids in plasma [28].

HFD treatment significantly reduced the level of acetic and butyric acid compared with control ($P < 0.05$). Isobutyric acid in HFD-fed mice revealed the same tendency. In addition, HFD significantly decreased total SCFAs compared with control ($P < 0.05$) (Fig. S1). MAP significantly increased the concentration of total SCFAs compared with HFD ($P < 0.05$), mainly via the increment of acetic acid and isobutyric acid. No obvious difference was observed in the levels of propionic acid between HFD and MAP groups. It seems that MAP reduced HFD-induced obesity partly through regulating the levels of SCFAs.

HFD can lead to intestinal ecological disorders, intestinal barrier dysfunction, and increased permeability. Lipopolysaccharide (LPS) is released into the blood and binds to TLR4 on the cell membrane, activates AP-1 and NF-κB, and then stimulates the transcription of inflammatory factors after AP-1 and NF-κB migrate to the cell nucleus. Cani et al. [29] revealed the relationship between LPS and obesity. They injected a low dose of LPS into mice fed normal diet for 4 weeks, and the mice developed obesity. However, knocking out LPS receptor CD14 and injecting LPS again do not cause obesity in mice. It is suggested that obesity can be induced when intestinal microbiota disorders are followed by metabolic endotoxemia. Our preliminary mechanism study showed that MAP could inhibit LPS-induced migration and invasion of colon cancer cells [11]. In addition, an apple oligogalactan could inhibit the expression of COX-2 by suppressing LPS signal [30]. MAP may reduce HFD-induced obesity through decreasing the production of LPS and suppressing the activation of LPS/TLR-4 pathway.

Taken together, we then speculate that MAP first regulated imbalance of the intestinal microbiota induced by HFD, then influenced the levels of SCFAs and/or suppressed LPS/TLR-4 pathway, and, finally, reduced HFD-induced obesity.

In summary, the results herein demonstrated the antiobesity effect of MAP on HFD-treated C57BL/6J mice. We found MAP could decrease fat accumulation in adipose tissue and liver, and improve blood lipid level. MAP can significantly regulate HFD-induced intestinal microbiota imbalance, and reduce the number of T cells and macrophages in adipose tissue. The encouraging data and the precise signaling pathway should remain to be further elucidated. However, these results indicate that MAP has a potential in treatment for obesity.

Author contributions The experiments were conceived and designed by YL, WX, and QM, and performed by YL, WX, YS, YW, YT, YL, XG, and CS; the data were analyzed by WX, YS, and LL. The initial manuscript draft was written by YL, and critically revised by LL and QM. And all authors read and approved the final manuscript.

Compliance with ethical standards

Conflict of interest The authors declare that they have no conflict of interest.

References

1. Prospective Studies C, Whitlock G, Lewington S, Sherliker P, Clarke R, Emberson J, Halsey J, Qizilbash N, Collins R, Peto R (2009) Body-mass index and cause-specific mortality in 900 000 adults: collaborative analyses of 57 prospective studies. Lancet 373(9669):1083–1096. https://doi.org/10.1016/S0140-6736(09)60318-4

2. Ng M, Fleming T, Robinson M, Thomson B, Graetz N, Margono C, Mullany EC, Biryukov S, Abbafati C, Abera SF, Abraham JP, Abu-Rmeileh NM, Achoki T, AlBuhairan FS, Alemu ZA, Alfonso R, Ali MK, Ali R, Guzman NA, Ammar W, Anwari P, Banerjee A, Barquera S, Basu S, Bennett DA, Bhutta Z, Blore J, Cabral N, Nonato IC, Chang JC, Chowdhury R, Courville KJ, Criqui MH, Cundiff DK, Dabhadkar KC, Dandona L, Davis A, Dayama A, Dharmaratne SD, Ding EL, Durrani AM, Esteghamati A, Farzadfar F, Fay DF, Feigin VL, Flaxman A, Forouzanfar MH, Goto A, Green MA, Gupta R, Hafezi-Nejad N, Hankey GJ, Harewood HC, Havmoeller R, Hay S, Hernandez L, Husseini A, Idrisov BT, Ikeda N, Islami F, Jahangir E, Jassal SK, Jee SH, Jeffreys M, Jonas JB, Kabagambe EK, Khalifa SE, Kengne AP, Khader YS, Khang YH, Kim D, Kimokoti RW, Kinge JM, Kokubo Y, Kosen S, Kwan G, Lai T, Leinsalu M, Li Y, Liang X, Liu S, Logroscino G, Lotufo PA, Lu Y, Ma J, Mainoo NK, Mensah GA, Merriman TR, Mokdad AH, Moschandreas J, Naghavi M, Naheed A, Nand D, Narayan KM, Nelson EL, Neuhouser ML, Nisar MI, Ohkubo T, Oti SO, Pedroza A, Prabhakaran D, Roy N, Sampson U, Seo

H, Sepanlou SG, Shibuya K, Shiri R, Shiue I, Singh GM, Singh JA, Skirbekk V, Stapelberg NJ, Sturua L, Sykes BL, Tobias M, Tran BX, Trasande L, Toyoshima H, van de Vijver S, Vasankari TJ, Veerman JL, Velasquez-Melendez G, Vlassov VV, Vollset SE, Vos T, Wang C, Wang X, Weiderpass E, Werdecker A, Wright JL, Yang YC, Yatsuya H, Yoon J, Yoon SJ, Zhao Y, Zhou M, Zhu S, Lopez AD, Murray CJ, Gakidou E (2014) Global, regional, and national prevalence of overweight and obesity in children and adults during 1980–2013: a systematic analysis for the Global Burden of Disease Study 2013. Lancet 384(9945):766–781. https://doi.org/10.1016/S0140-6736(14)60460-8

3. Collaboration NCDRF (2016) Trends in adult body-mass index in 200 countries from 1975 to 2014: a pooled analysis of 1698 population-based measurement studies with 19.2 million participants. Lancet 387(10026):1377–1396. https://doi.org/10.1016/s0140-6736(16)30054-x

4. Kinlen D, Cody D, O'Shea D (2018) Complications of obesity. QJM 111(7):437–443. https://doi.org/10.1093/qjmed/hcx152

5. Apovian CM (2016) Obesity: definition, comorbidities, causes, and burden. Am J Manag Care 22(7 Suppl):s176–s185

6. Noncommunicable Diseases Progress Monitor, 2017 (2017) World Health Organization (WHO), p 231. https://www.who.int/nmh/publications/ncd-progress-monitor-2017/en/(2017)

7. Bäckhed F, Ding H, Wang T, Hooper LV, Koh GY, Nagy A, Semenkovich CF, Gordon JI (2004) The gut microbiota as an environmental factor that regulates fat storage. Proc Natl Acad Sci USA 101(44):15718–15723. https://doi.org/10.1073/pnas.0407076101

8. Ridaura VK, Faith JJ, Rey FE, Cheng J, Duncan AE, Kau AL, Griffin NW, Lombard V, Henrissat B, Bain JR, Muehlbauer MJ, Ilkayeva O, Semenkovich CF, Funai K, Hayashi DK, Lyle BJ, Martini MC, Ursell LK, Clemente JC, Van Treuren W, Walters WA, Knight R, Newgard CB, Heath AC, Gordon JI (2013) Gut microbiota from twins discordant for obesity modulate metabolism in mice. Science 341(6150):1241214. https://doi.org/10.1126/science.1241214

9. Lazar V, Ditu LM, Pircalabioru GG, Picu A, Petcu L, Cucu N, Chifiriuc MC (2019) Gut microbiota, host organism, and diet trialogue in diabetes and obesity. Front Nutr 6:21. https://doi.org/10.3389/fnut.2019.00021

10. Wang S, Li Q, Zang Y, Zhao Y, Liu N, Wang Y, Xu X, Liu L, Mei Q (2017) Apple polysaccharide inhibits microbial dysbiosis and chronic inflammation and modulates gut permeability in HFD-fed rats. Int J Biol Macromol 99:282–292. https://doi.org/10.1016/j.ijbiomac.2017.02.074

11. Zhang D, Li YH, Mi M, Jiang FL, Yue ZG, Sun Y, Fan L, Meng J, Zhang X, Liu L, Mei QB (2013) Modified apple polysaccharides suppress the migration and invasion of colorectal cancer cells induced by lipopolysaccharide. Nutr Res 33(10):839–848. https://doi.org/10.1016/j.nutres.2013.06.004

12. Van Heek M, Compton DS, France CF, Tedesco RP, Fawzi AB, Graziano MP, Sybertz EJ, Strader CD, Davis HR Jr (1997) Diet-induced obese mice develop peripheral, but not central, resistance to leptin. J Clin Investig 99(3):385–390. https://doi.org/10.1172/JCI119171

13. Cole JR, Wang Q, Cardenas E, Fish J, Chai B, Farris RJ, Kulam-Syed-Mohideen AS, McGarrell DM, Marsh T, Garrity GM, Tiedje JM (2009) The Ribosomal Database Project: improved alignments and new tools for rRNA analysis. Nucleic Acids Res 37(database issue):D141–D145. https://doi.org/10.1093/nar/gkn879

14. Quast C, Pruesse E, Yilmaz P, Gerken J, Schweer T, Yarza P, Peplies J, Glockner FO (2013) The SILVA ribosomal RNA gene database project: improved data processing and web-based tools. Nucleic Acids Res 41(database issue):D590–D596. https://doi.org/10.1093/nar/gks1219

15. Schloss PD, Gevers D, Westcott SL (2011) Reducing the effects of PCR amplification and sequencing artifacts on 16S rRNA-based studies. PLoS One 6(12):e27310. https://doi.org/10.1371/journal.pone.0027310

16. Jiang XT, Peng X, Deng GH, Sheng HF, Wang Y, Zhou HW, Tam NF (2013) Illumina sequencing of 16S rRNA tag revealed spatial variations of bacterial communities in a mangrove wetland. Microb Ecol 66(1):96–104. https://doi.org/10.1007/s00248-013-0238-8

17. Vajro P, Paolella G, Fasano A (2013) Microbiota and gut-liver axis: their influences on obesity and obesity-related liver disease. J Pediatr Gastroenterol Nutr 56(5):461–468. https://doi.org/10.1097/MPG.0b013e318284abb5

18. Seo M, Inoue I, Tanaka M, Matsuda N, Nakano T, Awata T, Katayama S, Alpers DH, Komoda T (2013) Clostridium butyricum MIYAIRI 588 improves high-fat diet-induced non-alcoholic fatty liver disease in rats. Dig Dis Sci 58(12):3534–3544. https://doi.org/10.1007/s10620-013-2879-3

19. Turnbaugh PJ, Ley RE, Mahowald MA, Magrini V, Mardis ER, Gordon JI (2006) An obesity-associated gut microbiome with increased capacity for energy harvest. Nature 444(7122):1027–1031. https://doi.org/10.1038/nature05414

20. Ley RE, Backhed F, Turnbaugh P, Lozupone CA, Knight RD, Gordon JI (2005) Obesity alters gut microbial ecology. Proc Natl Acad Sci USA 102(31):11070–11075. https://doi.org/10.1073/pnas.0504978102

21. Boerner BP, Sarvetnick NE (2011) Type 1 diabetes: role of intestinal microbiome in humans and mice. Ann N Y Acad Sci 1243:103–118. https://doi.org/10.1111/j.1749-6632.2011.06340.x

22. Daien CI, Pinget GV, Tan JK, Macia L (2017) Detrimental impact of microbiota-accessible carbohydrate-deprived diet on gut and immune homeostasis: an overview. Front Immunol 8:548. https://doi.org/10.3389/fimmu.2017.00548

23. Bonder MJ, Kurilshikov A, Tigchelaar EF, Mujagic Z, Imhann F, Vila AV, Deelen P, Vatanen T, Schirmer M, Smeekens SP, Zhernakova DV, Jankipersadsing SA, Jaeger M, Oosting M, Cenit MC, Masclee AA, Swertz MA, Li Y, Kumar V, Joosten L, Harmsen H, Weersma RK, Franke L, Hofker MH, Xavier RJ, Jonkers D, Netea MG, Wijmenga C, Fu J, Zhernakova A (2016) The effect of host genetics on the gut microbiome. Nat Genet 48(11):1407–1412. https://doi.org/10.1038/ng.3663

24. Wang LL, Guo HH, Huang S, Feng CL, Han YX, Jiang JD (2017) Comprehensive evaluation of SCFA production in the intestinal bacteria regulated by berberine using gas-chromatography combined with polymerase chain reaction. J Chromatogr B Anal Technol Biomed Life Sci 1057:70–80. https://doi.org/10.1016/j.jchromb.2017.05.004

25. Albenberg LG, Wu GD (2014) Diet and the intestinal microbiome: associations, functions, and implications for health and disease. Gastroenterology 146(6):1564–1572. https://doi.org/10.1053/j.gastro.2014.01.058

26. Psichas A, Sleeth ML, Murphy KG, Brooks L, Bewick GA, Hanyaloglu AC, Ghatei MA, Bloom SR, Frost G (2015) The short chain fatty acid propionate stimulates GLP-1 and PYY secretion via free fatty acid receptor 2 in rodents. Int J Obes (Lond) 39(3):424–429. https://doi.org/10.1038/ijo.2014.153

27. Perry RJ, Peng L, Barry NA, Cline GW, Zhang D, Cardone RL, Petersen KF, Kibbey RG, Goodman AL, Shulman GI (2016) Acetate mediates a microbiome-brain-beta-cell axis to promote metabolic syndrome. Nature 534(7606):213–217. https://doi.org/10.1038/nature18309

28. Carmen GY, Victor SM (2006) Signalling mechanisms regulating lipolysis. Cell Signal 18(4):401–408. https://doi.org/10.1016/j.cellsig.2005.08.009

29. Cani PD, Amar J, Iglesias MA, Poggi M, Knauf C, Bastelica D, Neyrinck AM, Fava F, Tuohy KM, Chabo C, Waget A, Delmee E, Cousin B, Sulpice T, Chamontin B, Ferrieres J, Tanti JF, Gibson GR, Casteilla L, Delzenne NM, Alessi MC, Burcelin R (2007) Metabolic endotoxemia initiates obesity and insulin resistance. Diabetes 56(7):1761–1772. https://doi.org/10.2337/db06-1491

30. Li Y, Fan L, Sun Y, Zhang D, Yue Z, Niu Y, Meng J, Yang T, Liu W, Mei Q (2013) An apple oligogalactan suppresses endotoxin-induced cyclooxygenase-2 expression by inhibition of LPS pathways. Int J Biol Macromol 61:75–81. https://doi.org/10.1016/j.ijbiomac.2013.06.048